## Title

Synthesis and evaluation of vitamin D receptor-mediated activities of cholesterol and vitamin D metabolites



## Authors

Teske, Kelly A
Bogart, Jonathon W
Sanchez, Luis M
et al.

## Publication Date

2016-02-01

## DOI

10.1016/j.ejmech.2016.01.002

Peer reviewed

HHS Public Access

Author manuscript

*Eur J Med Chem*. Author manuscript; available in PMC 2017 February 15.

Published in final edited form as:

*Eur J Med Chem*. 2016 February 15; 109: 238–246. doi:10.1016/j.ejmech.2016.01.002.

# Synthesis and Evaluation of Vitamin D Receptor-Mediated Activities of Cholesterol and Vitamin D Metabolites

**Kelly A. Teske**, **Jonathan W. Bogart**, **Luis M. Sanchez**, **Olivia B. Yu**, **Joshua V. Preston**, **James M. Cook**, **Nicholas R. Silvaggi**, **Daniel D. Bikle**, and **Leggy A. Arnold***

Department of Chemistry and Biochemistry and Milwaukee Institute for Drug Discovery, University of Wisconsin, Milwaukee, Milwaukee, Wisconsin 53211, United States

## Abstract

A systematic study with phase 1 and phase 2 metabolites of cholesterol and vitamin D was conducted to determine whether their biological activity is mediated by the vitamin D receptor (VDR). The investigation necessitated the development of novel synthetic routes for lithocholic acid (LCA) glucuronides (Gluc). Biochemical and cell-based assays were used to demonstrate that hydroxylated LCA analogs were not able to bind VDR. This excludes VDR from mediating their biological and pharmacological activities. Among the synthesized LCA conjugates a novel VDR agonist was identified. LCA Gluc II increased the expression of CYP24A1 in DU145 cancer cells especially in the presence of the endogenous VDR ligand $1,25(OH)_2D_3$. Furthermore, the methyl ester of LCA was identified as novel VDR antagonist. For the first time, we showed that calcitroic acid, the assumed inactive final metabolite of vitamin D, was able to activate VDR-mediated transcription to a higher magnitude than bile acid LCA. Due to a higher metabolic stability in comparison to vitamin D, a very low toxicity, and high concentration in bile and intestine, calcitroic acid is likely to be an important mediator of the protective vitamin D properties against colon cancer.

### Keywords

Vitamin D Receptor; $1,25(OH)_2D_3$; metabolites; lithocholic acid; calcitroic acid; CYP24A1; DU145

## Introduction

Many biological activities of vitamin D, once converted to calcitriol ($1,25(OH)_2D_3$), are mediated by the vitamin D receptor (VDR, NR1I1), a ligand inducible transcription factor belonging to the superfamily of nuclear receptors (NRs)[1]. When $1,25(OH)_2D_3$ binds VDR, it undergoes a conformational change and initiates a cascade of events including the association of its heterodimeric partner, retinoid X receptor (RXR), followed by the recruitment of specific coactivators needed for transcription [2]. Ligand activated VDR has been shown to regulate the expression of VDR target genes involved in calcium homeostasis, immunity, and cellular growth and differentiation. In addition to its role in

*Corresponding author: arnold2@uwm.edu.

vitamin D physiology, VDR has been shown to bind bile acids and act as sensor for elevated concentrations of bile acids in the intestine [3]. Bile acids are end products of hepatic cholesterol catabolism and act as emulsifiers for ingestion and intestinal absorption of hydrophobic nutrients like cholesterol, fatty acids and lipid-soluble vitamins like vitamin D. Primary bile acids are produced from cholesterol in the liver through a series of enzymatic reactions catalyzed by $P_{450}$ enzymes followed by their secretion in the bile as glycine or taurine conjugates, where they assist in lipid digestion and absorption [4]. Most bile acids are reabsorbed in the intestine and recirculate to the liver, while others are converted to secondary bile acids, such as lithocholic acid (LCA) [5]. LCA is poorly reabsorbed into the enterohepatic circulation and can pass into the colon. At higher concentrations, LCA is toxic and has been linked to the development of liver disease and colorectal cancer [6, 7]. VDR plays an important role in maintaining bile homeostasis by inducing a LCA detoxification mechanism in the liver and intestine through the upregulation of CYP3A4 [8]. The crystallographic structure of VDR with LCA has been solved for both rVDR[9] and zVDR [10]. The zVDR crystallographic study revealed the necessity of a second LCA, which anchors to VDR by forming direct H-bonds at a considerably lower affinity compared to the usual ligand binding site but importantly stabilizes the active protein conformation. These studies suggest that other LCA metabolites might have stronger interactions with VDR than LCA, thus many LCA-derived ligands have been synthesized and investigated [11, 12]. The results showed that esterification of the LCA side chain carboxyl group with methyl, ethyl, and benzyl moieties resulted in very weak VDR agonists. However, esterification of the C3 hydroxyl group (LCA acetate) exhibited a 30-fold improved agonistic VDR-mediated transcriptional activity in comparison to LCA [11]. In colon cancer cells and mouse intestine, LCA acetate upregulated CYP3A significantly more than LCA, suggesting that LCA analogs could be developed into chemoprevention against colorectal cancer.

Similar to the negative feedback loop responsible for the catabolic breakdown of LCA by CYP3A4, $1,25(OH)_2D_3$ metabolism is mediated by the VDR target gene, CYP24A1 [13]. Major catabolism of $1,25(OH)_2D_3$ occurs at the secosteroid aliphatic chain either forming C24-oxidation pathway products or C23-hydroxylation pathway products [14]. The final product of the 23-hydroxylation pathway is $1,25(OH)_2$D-26,23-lactone that exhibit antagonistic VDR activities *in vivo* [15]. The final metabolite formed by the C24-oxidation pathway is the bile excretory product calcitroic acid. CYP24A1 is induced greatly by $1,25(OH)_2D_3$ in many different cancer cells including prostate cancer cells DU145 [16]. The resulting fast metabolism of $1,25(OH)_2D_3$ reduces its ability to induce cancer cell growth inhibition [17]. However, many aspects of this pathway are still unknown, especially the role of vitamin D metabolites. Herein, we report the systematic evaluation cholesterol and vitamin D metabolites in respect to VDR binding, modulation of VDR-mediated transcription, and toxicity.

## Results and Discussion

The following compounds depicted in Figure 1 were investigated in this study.

These include identified VDR agonists such as LCA, LCA acetate, and LCA methyl ester (LCME) [11]. Secondly, we investigated vitamin D metabolite calcitroic acid [13], and

cholesterol phase 1 metabolites ursodeoxycholic acid (UDCA), an FDA approved drug against primary biliary cirrhosis [18], cholic acid (CA) a treatment for bile acid synthesis disorders due to enzymatic effects [19], deoxycholic acid (DCA) used for the reduction of fat under the chin [20], chenodeoxycholic acid (CDCA) a treatment against gallstones [21], and hyodeoxycholic acid (HDCA), which is not marketed but has a similar activities to that of CDCA. In addition, phase 2 metabolites were studied such as glycolithocholic acid (GLCA), taurolithocholic acid (TLCA), sulfonolithocholic acid (SLCA), lithocholic acid glucuronides I and II (LCA Gluc I and II).

## Chemistry

LCA derivatives and metabolites, which are not commercially available were synthesized from LCA or LCME. LCA was the starting material used to synthesize LCA acetate and SLCA (Scheme 1). A base-catalyzed esterification reaction using 4-dimethylaminopyridine and acetyl chloride produced LCA acetate in a 95% yield. To obtain SLCA, sulfuric acid and acetic anhydride in pyridine were used, as opposed to the reported method using pyridine sulfur trioxide to make sulfonate steroids [22, 23]. The final product was converted into the corresponding ammonium salt using 25% ammonia acetate at 0°C to obtain the final product in a 97% yield.

For the synthesis of LCA Gluc I and II (Scheme 2), LCA methyl ester (LCME) was used as starting material. A Koenigs-Knorr condensation reaction of LCME with acetobromo-α-D-glucuronic acid methyl ester in the presence of $CdCO_3$ in dry benzene gave LCME Gluc I [24]. The β-glycosidic linkage with LCA methyl ester at the C-3 position was confirmed by $^1$HNMR. Hydrolysis with sodium hydroxide afforded the final product, LCA Gluc I, in an overall yield of 61%. LCA Gluc II was synthesized in four steps starting with the protection of LCME with *t*-butyldimethylsilylether (TBS). Hydrolysis of LCME-TBS afforded the corresponding carboxylic acid, LCA-TBS. Next, glucuronic acid was converted into a tetrabutylammonium salt (1) (Scheme 3), which not only protected the free carboxyl group but also rendered it soluble in organic solvents [25].

In a one pot reaction, LCA-TBS was activated with 1,1'-carbonyldiimidazole followed by the addition of tetrabutylammonium glucoronate (1). The reaction was quenched with acetic acid to produce LCA-TBS Gluc II. To avoid accidental cleavage of the coupled sugar ring, deprotection of the TBS group was accomplished under neutral conditions with tetrabutylammonium fluoride as oppose to acidic conditions. This reaction was quenched with water to yield the final product, LCA Gluc II, which was further purified by silica gel column chromatography to remove any unreacted LCA followed by recrystallization in EtOH to yield about 40 mg of product in an overall yield of 10%. Although this multistep synthesis produced little product, it was beneficial to have the sugar as the donor and LCA as the acceptor molecule since it omitted unnecessary protection and deprotection of the sugar hydroxyl groups.

## Biological Evaluation

Each compound was initially evaluated with a VDR–coactivator binding assay using a fluorescently labeled SRC2-3 coactivator peptide and recombinantly expressed VDR-LBD [26]. The results are summarized in Table 1.

LCME, LCA acetate, and calcitroic acid were not able to support the VDR-LBD recruitment of the SRC2-3 labeled coactivator peptide in this assay and even LCA, with a reported cellular activity of approximately 10 μM, exhibited a limited agonistic activity of greater than 50 μM [3]. The presence of two VDR binding sites for LCA might be responsible for the weak agonistic binding observed in this assay [10]. However, the VDR-SRC2-3 binding was inhibited by LCA with an $IC_{50}$= 13.6 ± 4.6 μM, while the introduction of a methyl ester (LCME) rendered the molecule inactive. LCA acetate had a similar inhibitor potency than LCA, whereas calcitroic acid was approximately six times more potent with an $IC_{50}$= 2.29 ± 0.43 μM. Obviously, the recruitment of SRC2-3 by VDR-LBD is sensitive to any three-dimensional protein changes induced by ligand binding. For instance, crystal structures of VDR with $1,25(OH)_2D_3$ or LCA showed different conformations of coactivator peptide MED1 [9]. The specificity of coregulator recruitment induced by VDR ligands using this and other binding assays has been reported [27]. Thus, LCA acetate and calcitroic acid and to a lesser extent LCA induce a three dimensional VDR conformation that did not enable SRC2 to bind VDR.

In addition, two cell-based assays were conducted in HEK-293T kidney cells. For the VDR transcription assay, a CMV-VDR-Gal4 fusion plasmid and a luciferase reporter plasmid with a 4×UAS promoter were over expressed. The 2-hybrid assay utilized three plasmids: a fusion plasmid of coactivator SRC1 and a GAL4 DNA binding domain, a fusion plasmid of VDR LBD and VP16, and a luciferase reporter plasmid with a 4×UAS promoter repeat. The assay enables the evaluation of ligand-dependent VDR recruitment of SRC1 in cells. The transcription and VDR–SRC1 binding efficacy induced by VDR ligands was normalized to the response of 10 nM $1,25(OH)_2D_3$. The compound cytotoxicity was determined in HEK293T cells by cellular ATP quantification.

In contrast to the VDR–SRC2 interaction, VDR agonist LCA promoted the cellular interaction between VDR and SRC1 with an $EC_{50}$ value of 2.14 ± 1.03 μM. In comparison to the binding efficacy of $1,25(OH)_2D_3$, LCA only partially agonized VDR with an efficacy of 39%. When competing with $1,25(OH)_2D_3$, LCA showed weak inhibition in the 34-47 μM range, which was likely caused by increased cell death at higher concentration due to its moderate toxicity. Analog LCME did not activate transcription and exhibited similar toxicity as LCA. However, LCME inhibited VDR–SRC1 recruitment at significantly lower concentrations with an $IC_{50}$ value of 15.1 ± 5.12 μM. Thus LCME behaves like a VDR antagonist supporting earlier results with VDR antagonist GW0742 that VDR ligand carboxylic esters antagonize transcription more strongly than their corresponding carboxylic acids [28]. The reported VDR agonist LCA acetate exhibited an $EC_{50}$ value of 1.49 ± 0.65 μM. No inhibition of VDR–SRC1 binding in the presence of $1,25(OH)_2D_3$ was observed in cells. The efficacy of LCA acetate was 94% with respect to $1,25(OH)_2D_3$. Importantly, calcitroic acid exhibited the highest agonistic potency among all metabolites investigated

with an $EC_{50}$ value of 0.87 ± 0.29 μM. The efficacy, however, was lower than LCA acetate but higher than LCA at 55% with respect to $1,25(OH)_2D_3$.

LCA phase 1 metabolites with hydroxyl groups attached on the B and C rings did not interact with VDR at concentrations comparable to their concentration in the intestine (250 μM in upper ileum to 1 mM in lower ileum) [29]. Although not toxic, these metabolites did not promote or inhibit VDR-coactivator interactions or mediate VDR transcription. The results could be attributed to the additional hydroxyl groups in what is typically a hydrophobic region of VDR ligands. The VDR-LBD pocket is mostly hydrophobic with hydrogen bonding occurring at the outer ends of the pocket. Therefore, hydroxyl groups in that hydrophobic region can promote unfavorable binding.

The investigation of LCA conjugates demonstrated their inability to promote the interaction between VDR-LBD and coregulator peptide SRC2-3 in contrast to $1,25(OH)_2D_3$. However, LCA Gluc II was able to bind VDR but induced a significant conformational change that excluded SRC2-3 binding to VDR with an $IC_{50}$ of 2.86 ± 0.55 μM. Other metabolites moderately inhibited the VDR–SRC2-3 interaction with $IC_{50}$ values ranging between 14.5-40 μM. In cells, LCA conjugates LCA Gluc I and LCA Gluc II promoted the interaction between VDR and SRC1. The observed $EC_{50}$ values were 20.5 ± 13.1 μM and 6.52 ± 2.60 μM, respectively. These concentrations are in the range of physiological concentrations of bile acids, which vary between 2 mM to 10 mM in the small intestine [29]. In the presence of $1,25(OH)_2D_3$, no inhibition of VDR–SRC1 binding was observed. In addition, a transcription assay using a hVDR-Gal4 and luciferase reporter plasmid confirmed the agonistic activity of LCA Gluc I and LCA Gluc II. The efficacy for LCA Gluc II in this assay was significantly higher than LCA Gluc I with (70%) and (55%), respectively. Thus the interaction between VDR and SRC1 is biologically relevant in contrast to VDR–SRC2 binding. As a control experiment, HEK293 cells were transfected with a PPARα-Gal4 plasmid in combination with a luciferase reporter plasmid and treated with LCA Gluc I or LCA Gluc II. Quantification of luminescence revealed no activation of transcription for the PPARα-Gal4 system suggesting that LCA Gluc I and Gluc II do not interfere with the Gal4-Luc detection system in general and that both compounds selectively agonize VDR in comparison to nuclear receptors like PPARα.

Transcriptional modulation mediated by VDR in the presence of cholesterol and vitamin D metabolites was confirmed in non-transfected DU145 cells. In comparison to $1,25(OH)_2D_3$, the ability to induce VDR target gene CYP24A1 was quantified by qRT-PCR. Therefore, selected VDR ligands at a concentration of 7.5 μM were incubated in the absence and presence of 20 nM $1,25(OH)_2D_3$ for 18 hours. The results are illustrated in Figure 2.

As reported for colon cancer cell line SW480, a strong induction of CYP24A1 in DU145 cells was observed in the presence of $1,25(OH)_2D_3$, whereas the transcriptional activation in relationship to $1,25(OH)_2D_3$ was less pronounced for LCA acetate and LCA with 24% and 6%, respectively [12]. For the first time, we could show that calcitroic acid, which is thought to be the inactive final metabolic product of $1,25(OH)_2D_3$, was able to induce VDR target gene CYP24A1. Found in high concentration in the liver and secreted into the duodenum via the gallbladder, calcitroic acid and lithocholic acid are likely to have similar functions [30].

Thus, calcitroic acid because of its high concentration in the intestine and superior ability to induce transcription in comparison to LCA, might play a very important role in the detoxification of LCA mediated by VDR target gene CYP3A [3]. The agonistic effect of LCA Gluc I, observed in the transcription assays, could not be recapitulated as gene up-regulation of CYP24A1 in DU145 cells, however, LCA Gluc II induced a weak induction of CYP24A1, which was more pronounced in the presence $1,25(OH)_2D_3$. Interestingly, none of the other VDR agonists activated VDR in a synergistic way, thus the interaction between VDR and LCA Gluc II might in addition to VDR binding promote R×R heterodimerization. With respect to intestinal detoxification, LCA Gluc II in addition to LCA might signal high concentrations of LCA conjugates via VDR to induce the transcription of enzymes that initiated their catabolism.

## Conclusion

The LCA-based phase 1 metabolites investigated herein bearing hydroxyl functions are not hydrophobic enough to interact with VDR. Thus their biological and pharmacological activity is not expected to be mediated by VDR. Furthermore, we confirmed and quantified the reported cellular agonistic activity of LCA and LCA acetate and identified LCME as a novel VDR antagonist. Calcitroic acid, an assumed inactivated metabolite of $1,25(OH)_2D_3$, was shown to have potent agonistic activity with respect to VDR. Based on its ability to promote the catabolism of $1,25(OH)_2D_3$ in prostate cancer cells via upregulation of CYP24A1, calcitroic acid might be able to upregulate CYP3A in the colon thus playing a major role in intestinal detoxification and parallel mediate the vitamin D protective effect against colon cancer. Further investigations in this area are currently being carried out and include a comprehensive evaluation of biological functions and distribution of calcitroic acid in the gut. Finally, LCA glucuronide (LCA Gluc II) was identified as novel endogenous VDR agonist that enables signaling of high concentrations of bile acid conjugates. This is especially important based on the fact more than 85% of bile acids are conjugated in the gut. The observed synergistic activation of VDR in the presence of $1,25(OH)_2D_3$ might enable LCA Gluc II to enhance LCA signaling in the intestine and accelerate the production of metabolic enzymes for tissue protection.

## Experimental Section

### Chemical Compounds and Synthesis

Reagents including lithocholic acid, lithocholic methyl ester and taurolithocholic acid were purchase from Sigma-Aldrich while glycolithocholic acid was purchased from Santa Cruz Biotechnology. Calcitroic acid was purchased from Toronto Research Chemicals. Synthesized compounds were either purified via recrystallization or normal phase flash chromatography (SPI Biotage, silica gel 230-400 mesh). Molecular masses were determined with a Shimadzu 2020 LC-MS (single quadrupole) instrument using direct injection. NMR spectra were recorded on a Bruker 500MHz of 300MHz instrument with samples diluted in either $CDCl_3$ or DMSO-$D_6$. Chemical shifts are reported in δ (parts per million: ppm) by reference to the hydrogenated residues of the deuterated solvent as an internal standard

($CDCl_3$: δ= 7.24 ppm ($^1$H-NMR) and δ= 77 ppm ($^{13}$C-NMR) and DMSO-$D_6$: δ= 2.50 ppm ($^1$H-NMR) and δ= 39.5 ppm ($^{13}$C-NMR).

**LCA Acetate—**Lithocholic acid (0.5 g, 1.3 mmol), was dissolved in dry pyridine (10mL) under $N_2$ gas and cooled to 0°C. 4-dimethylaminopyridine (0.02 g, 0.13 mmol) and acetyl chloride (1.1 mL, 16 mmol) were added to the solution. The reaction was stirred at room temperature and monitored by TLC using EtOAc-Hexanes-MeOH (4:1:1, v/v/v) and cerium molybdate as a developing stain. After 1 hour, water (3 mL) was added and the solution was evaporated under reduced pressure. Dichloromethane (15 mL) was used to dissolve the residue, which was subsequently washed with saturated aqueous NaCl (20 mL) and water (15 mL). The organic phase was dried over $Na_2SO_4$, then filtered and evaporated to dryness. The crude product was co-evaporated with toluene (10 mL ×2), ethanol (10 mL ×2), acetonitrile (10 mL × 2) and DCM (10 mL × 2) in order to remove traces of pyridine and purified by silica gel chromatography with $CH_3OH/CH_2Cl_2$ mixture (0%-5% strong). Yield: 95%; $^1$H-NMR (300 MHz) ($CDCl_3$) δ 4.75 (m, 1H, H-3), 2.05 (s, 3H, -$CH_3$, Ac), 0.95 (m, 6H, H-18/19, 21), 0.67 (s, 3H, H-18/19); $^{13}$C NMR δ 178.57, 170.72, 74.43, 56.51, 55.99, 42.75, 41.89, 40.42, 40.16, 35.79, 35.35, 35.03, 34.58, 32.25, 31.06, 29.69, 28.18, 26.32, 23.33, 20.83, 18.55, 18.28, 12.05; MS DUIS (¯ve) calcd. *m/z* for $C_{26}H_{42}O_4$ [(M)] 418.3, found [$(M-1)^-$] 417.4.

**LCA Sulfonate—**Sulfuric acid (0.16 mL, 3 mmol) and acetic anhydride (0.28 mL, 3 mmol) were mixed with dry pyridine (5 mL) and after 5 minutes of stirring at 50-55°C a solution of lithocholic acid in 2 mL of pyridine was added. The mixture was stirred for 30 minutes at the same conditions, cooled to 0°C, and 25% ammonia water (0.74 mL) was added. After 15 minutes of stirring, the precipitate was filtered and the filtrate was placed on a rotary evaporator for concentrating. The product isolated was not purified further. Yield: 97%; $^1$H-NMR (300 MHz) (DMSO-$D_6$) δ 3.96 (m, 1H, H-3), 0.88 (m, 6H, H-18/19, 21), 0.61 (s, 3H, H-18/19); $^{13}$C NMR δ 175.18, 75.98, 56.41, 55.93, 42.66, 35.77, 35.47, 35.24, 24.53, 33.77, 31.21, 31.08, 28.16, 27.27, 26.52, 24.31, 23.65, 20.85, 18.59, 12.34; $^{13}$CDEPT-135 δ Negative (−) $CH_2$: 76.05, 56.42, 55.94, 42.06, 40.33, 35.82, 35.51, 24.31, 18.59, 12.34 Positive (+) CH and $CH_3$: 40.09, 35.29, 33.80, 31.21, 31.13, 28.16, 27.27, 26.53, 23.64, 20.85; MS DUIS (¯ve) calcd. *m/z* for $C_{24}H_{40}O_6S$ [(M)] 456.3, found [$(M-1)^-$] 455.4.

**LCME O-glucuronide I—**To a solution of lithocolic methyl ester (400 mg) in anhydrous benzene (16 mL) was added cadmium carbonate (400 mg), acetobromo-α-D-glucuronic acid methyl ester (400 mg) and a quantity of molecular sieves (400 mg). The mixture was stirred at reflux. After 1 hour and 3 hours, additional quantities of acetobromo-α-D-glucuronic acid methyl ester (200 mg) and cadmium carbonate (200 mg) were added and the mixture stirred for 7 hours and was monitored by TLC using hexane-EtOAc-AcOH (50:50:1, v/v/v) and cerium molybdate as the developing stain. The precipitate was removed by filtration and washed with EtOAc. The filtrate and washings were combine and evaporated to dryness under reduced pressure and the oily residue was recrystallized in MeOH (5mL) to make white crystals. Yield: 43%; $^1$H-NMR (300 MHz) ($CDCl_3$) δ 5.28-5.24 (m,2H), 5.01-4.95 (t, 1H, J= 9Hz), 4.69-4.66 (d, 1H, J= 9Hz, anomeric), 4.06-4.03 (d, 1H, J= 9Hz), 3.78 (s, 3H,

Ac), 3.69 (s, 3H, Ac), 3.62 (m, 1H, H-3), 2.07, 2.04 (s, 9H, $COCH_3$), 0.92 (m, 6H, H-18/19, 21), 0.65 (s, 3H, H-18/19); $^{13}$C NMR δ 174.76, 170.21, 169.35, 169.28, 167.32, 99.57, 80.56, 72.61, 72.20, 71.57, 69.50, 56.28, 55.89, 52.82, 51.46, 42.70, 42.17, 40.30, 40.09, 35.81, 35.35, 35.09, 34.63, 33.99, 31.05, 30.99, 28.16, 27.09, 27.01, 26.23, 24.16, 23.35, 20.83, 20.71, 20.63, 20.51, 18.25, 12.01; MS DUIS ($^+$ve) calcd. *m/z* for $C_{38}H_{58}O_{12}$ [(M)] 706.4, found [(M+ 18 ($NH_4$))$^+$] 724.8.

**LCA O-glucuronide I—**To a solution of LCME *O*-glucuronide I (70 mg) in MeOH (8 mL) an aqueous solution of 2M NaOH was added dropwise until the mixture was basic (pH 14). The reaction was stirred at room temperature overnight and monitored by TLC using hexanes-EtOAc-AcOH (50:50:1, v/v/v) and cerium molybdate as the developing stain. After most of the solvent was removed by rotary evaporation, the reaction product was diluted with water, neutralized with 3M HCl and then evaporated to dryness. The residue was re-suspended in anhydrous EtOH (10 mL) and the insoluble material was filtered off and washed with EtOH. The combined filtrate was evaporated and the residue was recrystallized from MeOH resulting in white, flakey solid. Yield: 100%: $^1$H-NMR (300 MHz) (DMSO-$D_6$) δ 4.34-4.31 (d, 1H, J= 9Hz), 3.61-3.58 (d, 1H, J= 9Hz), 3.33-3.27 (2H, t, J= 9Hz), 3.20-3.14 (1H, t, J= 9Hz), 2.93 (m, 1H, H-3), 0.88 (m, 6H, H-18/19, 21), 0.61 (s, 3H, H-18/19); $^{13}$C NMR δ 175.30, 170.86, 101.33, 77.75, 76.55, 76.00, 73.65, 72.01, 56.45, 55.97, 51.65, 42.72, 41.86, 35.80, 35.29, 34.26, 31.13, 30.83, 28.17, 27.20, 26.85, 26.55, 24.31, 26.55, 24.31, 23.49, 20.86, 18.59, 12.32 ; MS DUIS ($^-$ve) calcd. *m/z* for $C_{30}H_{48}O_9$ [(M)] 552, found [(M-1)$^-$] 551.

**LCME-TBS—***T*o a solution of LCME (3 g, 0.0077 mol) and imidazole (3.74 g, 0.0231 mol, 3 equiv.) in dry DMF (28 mL) tert-butyldimethylsilyl chloride (3.48 g, 0.0231 mols, 3 equiv.) was added dropwise. The mixture was stirred overnight at room temperature and monitored by TLC using EtOAc-DCM- AcOH (5:95:1, v/v/v) and cerium molybdate as the developing stain. Upon completion, the reaction was diluted with water and extracted with DCM (25 mL × 3) and then dried using rotary evaporation. The resulting crude product was purified using silica gel chromatography using EtOAc-Hexanes with 1% AcOH (1% -20% strong). A white solid was isolated. Yield: 84%; $^1$H-NMR (300 MHz) ($CDCl_3$) δ 3.67 (s, 3H, Ac) 3.59 (m, 1H, H-3), 0.92 (m, 6H, H-18/19, 21), 0.90 (s, 9H, t-butyl-Si), 0.63 (s, 3H, H-18/19), 0.06 (s, 6H, 2$CH_3$-Si); $^{13}$C NMR δ 174.90, 135.15, 121.89, 72.85, 56.39, 55.93, 51.49, 42.70, 42.27, 40.20, 40.12, 36.90, 36.49, 35.84, 35.56, 35.36, 34.57, 31.57, 31.06, 31.00, 28.18, 27.28, 26.39, 25.97, 25.74, 24.20, 23.38, 20.79, 18.33, 18.24, 12.00; MS DUIS ($^+$ve) calcd. *m/z* for $C_{31}H_{56}O_3Si$ [(M)] 504, found [(M-TBDMS)]$^+$ 373 and [(M +1+imidazole)$^+$] 574.

**LCA-TBS—**LCME-TBS (3.25 g, 6.45 mmol) was dissolved in THF (20 mL) and to it 2M NaOH was added until it reached pH=10. The reaction was stirred at 75°C for 24 hours and monitored by TLC using EtOAc-Hexanes-AcOH (3:2:1, v/v/v) and cerium molybdate as the developing stain. Once complete, most of the solvent was removed by rotary evaporation. The reaction product was diluted with water and acidified with 3M HCl to pH=3. The solid formed was collected and purified by silica gel chromatography using EtOAc-Hexanes with 1% AcOH (1-20% strong). A white solid with low solubility in MeOH, EtOH and $CHCl_3$

was obtained. Yield: 64%; $^{1}$H-NMR (500 MHz) (DMSO-$D_6$) δ 8.45 (s, 1H, COOH), 3.58 (m, 1H, H-3), 0.88 (m, 6H, H-18/19, 21), 0.85 (s, 9H, t-butyl-Si), 0.61 (s, 3H, H-18/19), 0.02 (s, 6H, 2$CH_3$-Si); $^{13}$C NMR δ 175.14, 72.56, 56.45, 56.09, 42.80, 42.05, 37.11, 35.90, 35.49, 35.24, 34.62, 31.34, 31.24, 28.11, 27.26, 26.53, 26.28, 24.28, 23.62, 20.92, 18.65, 18.23, 12.36; MS DUIS (⁻ve) calcd. *m/z* for $C_{31}H_{54}O_3Si$ [(M)] 490.3, found [(M-1)$^-$] 489.4.

**Tetrabutylammonium Glucuronate (1)—**Glucuronic acid (2.9 g) was suspended in methanol (25 mL) to which tetrabutylammonium hydroxide 30-hydrate (12 g) was added. The mixture was stirred at room temperature for 1 hour until a clear solution resulted. The solvent was removed in a rotary evaporator at 40°C, thereby yielding a syrup. Addition of acetone (100 mL) resulted in precipitation of the tetrabutylammonium glucoronate. That salt was separated by filtration and washed with acetone. The filtrate and washings, on further concentration in a rotary evaporator, resulted in precipitation of more salt. A flakey, white solid was obtained. Yield: >95%; $^{1}$H-NMR (500MHz) (DMSO-$D_6$) δ 5.75- 5.72 (d, 1H, J= 9Hz), 4.50-4.58 (d, 1H, J= 6Hz), 3.86-3.58 (m, 4H,OHs), 3.19-3.14 (m, 8H), 1.57 (m, 8H), 1.37-1.25 (m, 8H), 0.96-0.91 (t, 12H, J= 7.5Hz); MS DUIS (⁻ve) calcd. *m/z* for $C_{22}H_{45}NO_7$ [(M)] 435.2, found [(M-tetrabutylammonium)$^-$] 193.

**LCA-TBS-O-glucuronide II—**LCA-TBS (1.0 g, 2.04 mmol) and 1,1'-carbonyldiimidazole (0.66 g, 4.08 mmol, 2 equiv.) were dissolved in dry pyridine (40 mL). The mixture was stirred at reflux overnight and was monitored by both TLC using EtOAc-Hexanes-AcOH (4:1:1, v/v/v) and cerium molybdate as a developing stain and mass spectrometry. The development of a peak at 542 *m/z* in the positive mode indicated the formation of LCA-TBS-imidazole coupled product. To the same reaction mixrure, tetrabutylammonium glucuronate (2.22 g, 5.1 mmol, 2.5 equiv.), dry pyridine (10 mL), and sodium hydride (15 mg, 0.04 mmol, 0.02 equiv.) were added and the reaction was stirred at 50°C for 5 hours. The reaction was monitored by TLC (same conditions as above) and mass spectrometry. The development of a peak at 666 *m/z* in the negative mode indicated the formation of LCA-TBS-*O*-glucuronide II product. The reaction was stopped by careful addition of water. After the solution was made acidic with acetic acid, the product was extracted with EtOAc (25mL × 3). The EtOAc layer was dried over $Na_2SO_4$ and then evaporated to dryness with a rotary evaporator. The final yellow oil was not purified and was directly used for the next reaction. Yield: >95% (crude); Crude sample: $^{1}$H-NMR (300 MHz) (DMSO-$D_6$) δ 4.69-4.67 (d, 2H, J= 6Hz anomeric), 3.47 (m, 1H, H-3), 0.89 (m, 6H, H-18/19, 21), 0.83 (s, 9H, t-butyl-Si), 0.63 (s, 3H, H-18/19), 0.07 (s, 6H, 2$CH_3$-Si); $^{13}$C NMR δ 178.36 (glucuronic acid COOH) and 175.73 (LCA COOR) MS DUIS (⁻ve) calcd. *m/z* for $C_{36}H_{62}O_9Si$ [(M)] 667, found [(M-1)$^-$] 666.

**LCA O-glucuronide II—**LCA-TBS-O-glucuronide II (1.3 g, 2.0 mmol) was dissolved in a 1.0M THF solution of tetrabutylammonium fluoride (1.66 mL, 3 equiv.). The reaction was stirred at 40°C for 2 days and was monitored by mass spectrometry with the disappearance of the starting material peak at 666 *m/z* in the negative mode. When complete, the reaction was quenched with addition of water and washed with EtOAc (3×). The EtOAc layer was dried over $MgSO_4$ and dried by rotary evaporation. The crude yellow oil re-suspended in EtOH and the insoluble solid was filtered and washed with EtOH. The filtrate was collected

and dried. The residue was then purified using silica gel chromatography with MeOH-EtOAc with 1%AcOH (0-60% strong) to remove the LCA impurity. Fractions containing the product were dried and then recrystallized with EtOH to produce a cream colored solid. Yield: 10%; $^{1}$H-NMR (300 MHz) (DMSO-$D_6$) δ 5.23-3.77 (m, 5H, sugar-ring protons), 3.46 (m, 1H, H-3), 2.28-2.22 (m, 0.88 (m, 6H, H-18/19, 21), 0.62 (s, 3H, H-18/19); $^{13}$DEPT-135 δ Negative (-) $CH_2$: 56.48, 40.25, 36.78, 35.64, 31.11, 30.86, 28.14, 27.38, 26.64, 20.89, Positive (+) CH and $CH_3$: 93.07, 89.76, 70.77, 70.34, 56.52, 42.01, 40.81, 40.53, 40.43, 40.25, 39.98, 39.70, 35.86, 35.21, 23.74, 19.02, 18.62, 12.34. MS DUIS (¯ve) calcd. *m/z* for $C_{30}H_{48}O_9$ [(M)] 552, found [$(M-1)^-$] 551.

## Biological Assay Protocols

**Reagents—**LG190178 (a VDR agonist) was synthesized following a published procedure and used as a positive control. 3-dibutylamino-1-(4-hexyl-phenyl)-propan-1-one (a VDR-coactivator inhibitor) was used as a second positive control and was synthesized using a previously published method. 1,25$(OH)_2D_3$ was purchased from Endotherm. The VDR-LBDmt DNA was provided by D. Moras[31] and cloned into pMAL-z2× vector (New England Biolabs). For a details on the expression and purification of VDR-LBD, see ref[27]. Alexa Fluor 647 Labeled SRC2-3 was synthesized by labeling SRC2-3 (CKKKENALLRYLLDKDDTKD) with cysteine-reactive Alexa Fluor 647 probe followed by reverse phase HPLC using a C18 column. VDR-CMV and CYP24A1-luciferase reporter plasmids were provide by D.D. Bikle, VP16-VDR-LBD and SRC1-GAL4 plasmid were provided by D.J. Mangelsdorf,[3] and hVDR-Gal4 was provided by S.D. Ayers.

**VDR Binding Determined by a Fluorescence Polarization (FP) Assay—**Was conducted in 384-well black polystyrene microplates (Corning, #3573). The assay solution contained buffer (25mM PIPES, 50mM NaCl (Fisher), and 0.01% NP-40, at pH 6.75), 0.1 μM VDR-LBD and 7.5 nM Alexa Fluor 647-labeled SRC2-3. For competitive inhibition, 0.75 μM LG190178 was also added to the solution. 30 mM stock solutions of synthesized compounds made in DMSO were serially diluted (1:3), and four 14 μL aliquots of each compound concentration was transferred to opaque 384-well polypropylene plates for storage. Small volume transfers were performed by a Tecan Freedom EVO liquid handling system using a 50H hydrophobic coated pin tool that carried 100 nL (V&P Scientific). To obtain a maximum concentration of 150 μM, 300 nl of each compound concentration was transferred into the 20 μl assay solution. Agonistic binding was determined in the absence of LG190178 while competitive inhibition binding was determine in the presence of LG190187. Fluorescence polarization was detected after 30 minutes at an emission/excitation wavelength of 635/685 nm (Alexa Fluor 647). LG190178 and DMSO were used as positive and negative controls in the agonistic binding assay, respectively. In the competitive inhibition binding assay 3-dibutylamino-1-(4-hexyl-phenyl)-propan-1-one was the positive control while DMSO was used as a negative control. Controls were measured within each plate to determine the z' factor, which assed the quality of the assay, and enable data normalization. Three independent experiments were carried out in quadruplicate, and data was analyzed using nonlinear regression with a variable slope (GraphPrism).

**Transcription Assays—**Human embryonic kidney (HEK) 293T cells were purchased (ATCC) and cultured in 75 $cm^2$ flasks (CellStar) coated in matrigel (BD Bioscience, #354234). Cells were grown in DMEM/High Glucose (Hyclone, #SH3024301) media to which non-essential amino acids (Hyclone, #SH30238.01), 10 mM HEPES (Hyclone, #SH302237.01), $5 \times 10^6$ units of penicillin and streptomycin (Hyclone, #SV30010), and 10% of heat inactivated fetal bovine serum (Gibco, #10082147) were added. For the assay, cells at 70-80% confluency were transfected by lipid-based methods where 2 mL of untreated DMEM/High Glucose media (without additives) containing: 1) 2-Hybrid assay: 5.0 μg of VP16-VDR-LBD plasmid, 4.0 μg of SRC1-GAL4 plasmid, 16 μg of a luciferase reporter plasmid or 2) transcription assay: 1.5 μg of hVDR-Gal4 plasmid and 16 μg of a 4×UAS luciferase reporter plasmid, Lipofectamine™ LTX (75 μl, Life Technologies, #15338020), and PLUS™ reagent (25 μl) was added to the flask. After 16 hours of incubation at 37°C with 5% $CO_2$, the cells were harvested with 3mL of 0.05% Trypsin (Hyclone, #SH3023601), added to 10mL of the assay buffer, DMEM/High Modified buffer without phenol red (Hyclone, #SH30284.01) containing all the above mentioned additives plus 10 mM sodium pyruvate and 2% percent charcoal treated FBS (Invitrogen, #12676-011) instead of HI FBS, and spun down for 2 minutes at 1000 rpm. The media was removed and cells were resuspended in the assay buffer, DMEM/High Modified buffer without phenol red. Prior to adding cells to sterile white, optical bottom 384-well plates (NUNC, #142762), plates were treated with 20 μL per well of a 0.25% matrigel solution. To each well, 20 μL of cells were added to yield a final concentration of 15,000 cells per well. After 4 hours, plated cells were treated with 100 nL of small molecules (1:3 serial dilution, with maximum final concentration at 150 μM) and controls (DMSO and 10 nM $1,25(OH)_2D_3$ ) which were added using a Tecan Freedom EVO liquid handling system with a 50H hydrophobic coated pin tool. In the competitive inhibition assay, $1,25(OH)_2D_3$ (10 nM) was also added to the assay wells containing small molecule. After 16 hours of incubation at 37°C with 5% $CO_2$, 20μL of Bright-Glo™ Luciferase Assay Kit (Promega, Madison, WI) was added to each well and luminescence was read. Controls were measured within each plate to determine the z' factor and to enable data normalization. Three independent experiments were performed in quadruplicate and data was analyzed using nonlinear regression with variable slope (GraphPrism).

**Cytotoxicity Assay—**Hek293T cells were plates according to the transcription assay protocol and 100 nL of serially diluted (1:3 in DMSO) small molecules (final maximum concentration at 150 μM) were transferred using a Tecan Freedom EVO liquid handling system with a 50H hydrophobic coated pin tool. The controls for the cytotoxicity assay used were 3-dibutylamino-1-(4-hexyl-phenyl)-propan-1-one (150 μM in DMSO, positive) and DMSO (negative). After 18 hours, assay plates were evaluated by adding 20 μL of Cell Titer-Glo™ Luminescence Assay Kit (Promega, Madison, WI) to each well and reading luminescence on a Tecan Infinite M1000 plate reader. Controls were measured within each plate to determine the z' factor and to enable data normalization. Three independent experiments were performed in quadruplicate and data was analyzed using nonlinear regression with variable slope (GraphPrism).

**Semi-quantitative Real Time-PCR—**Reagents and Instrumentation: The prostate cancer cell line, DU145, was purchased (ATCC) and in cultured in 75 $cm^2$ flasks (CellStar). Cells were grown in DMEM/High Glucose media to which non-essential amino acids, 10 mM HEPES, $5 \times 10^6$ units of penicillin and streptomycin, and 10% of heat inactivated fetal bovine serum were added. Cells at 80-90% confluency were harvested using 0.25% Trypsin, spun down in assay buffer, DMEM media without phenol red containing the above mentioned additives (section 4.2.5), at 1000 rpm for 2 minutes. The media was removed and the cells were resuspended in the assay buffer and transferred to 6 well plates coated in matrigel. Plates were incubated at 37°C overnight to allow the cells to settle and adhere to the plate. The next day, DMSO (0.03%), test compound (7.5 μM, LCA *O*-glucuronide I, LCA *O*-glucuronide II, Calcitroic acid, LCA) and $1,25(OH)_2D_3$ (20 nM) were added to their own well in the 6-well plate and incubated at 37°C for 18 hours. Small molecules were either in the presence or absence of $1,25(OH)_2D_3$. Cells were harvested according to literature using a QIAshredder (Qiagen) to lyse the cells and a RNAeasy kit (Qiagen) to isolate total RNA for each compound. RNA concentration was determine by UV at 260nm using the Tecan Infinite M1000 plate reader. A QuantiFast SYBR Green RT-PCR Kit (Qiagen) was used for the real time PCR following manufacturer's recommendations. Primers used in these studies are as follows: GAPDH FP 5'-ACCACAGTCCATGCCATCAC-3', GAPDH RP 5'-TCCACCACCCTGTTGCTGTA-3'; CYP24A1 FP 5'-CTTTGCTTCCTTTTCCCAGAAT-3'; CYP24A1 RP 5'-CGCCGTAGATGTCACCAGTC-3'; Real-time rt-PCR was carried out on a Mastercycler (Eppendorf). The ΔΔCt method was used to measure the fold change in gene expression of target gene, CYP24A1. Standard errors of mean were calculated from two biological independent experiments performed in triplicates. Significance was calculated using Dunnett ANOVA in GraphPrism.

## Supplementary Material

Refer to Web version on PubMed Central for supplementary material.

## Acknowledgement

This work was supported by the University of Wisconsin-Milwaukee, the University of Wisconsin Milwaukee Research Growth Initiative, the National Institutes of Health [R03 DA031090], the University of Wisconsin Milwaukee Research Foundation (Catalyst grant), the Lynde and Harry Bradley Foundation, the Richard and Ethel Herzfeld Foundation, and National Institutes of Health [RO1 AR050023].

## ABBREVIATIONS

| | |
|---|---|
| **VDR** | Vitamin D Receptor |
| **$1,25(OH)_2D_3$** | calcitriol |
| **NR** | nuclear receptors |
| **LCA** | lithocholic acid |
| **LCME** | lithocholic acid methyl ester |
| **UDCA** | ursodeoxycholic acid |

| | |
|---|---|
| **CA** | cholic acid |
| **DCA** | deoxycholic acid |
| **CDCA** | chenodeoxycholic acid |
| **HDCA** | hyodeoxycholic acid |
| **GLCA** | glycolithocholic acid |
| **TLCA** | taurolithocholic acid |
| **SLCA** | sulfonolithocholic acid |
| **LCA Gluc I** | lithocholic acid glucuronide I |
| **LCA Gluc II** | lithocholic acid glucuronide II |
| **Cyp24A1** | 24-hydroxylase gene |

## References


[1]. Mangelsdorf DJ, Thummel C, Beato M, Herrlich P, Schutz G, Umesono K, Blumberg B, Kastner P, Mark M, Chambon P, Evans RM. The Nuclear Receptor Superfamily: The Second Decade. Cell. 1995; 83:835–839. [PubMed: 8521507]

[2]. Glass CK, Rosenfeld MG. The coregulator exchange in transcriptional functions of nuclear receptors. Genes Dev. 2000; 14:121–141. [PubMed: 10652267]

[3]. Makishima M, Lu TT, Xie W, Whitfield GK, Domoto H, Evans RM. Vitamin D receptor as an intestinal bile acid sensor. Science. 2002; 296:1313–1316. [PubMed: 12016314]

[4]. Russell DW. The enzymes, regulation and genetics of bile acid synthesis. Annual Review of Biochemistry. 2003; 72:137–174.

[5]. Ridlon JM, Kang D-J, Hylemon PB. Bile salt biotransformations by human intestinal bacteria. J. Lipid Res. 2006; 47:241–259. [PubMed: 16299351]

[6]. Kim I, Morimura K, Shah Y, Yang Q, Ward JM, Gonzalez FJ. Spontaneous hepatocarcinogensis in farnesoid X receptor-null mice. Carcinogenesis. 2007; 28:940–946. [PubMed: 17183066]

[7]. Nagengast FM, Grubben MJ, Munster IPV. Role of biles acids in colorectal carcinogenesis. Eur. J. Cancer. 1995; 7-8:1067–1070. [PubMed: 7576993]

[8]. Cheng J, Fang Z-Z, Kim J-H, Krausz KW, Tanaka N, Chiang JYL, Gonzalez FJ. Intestinal CYP3A4 protects against lithocholic acid-induced hepatoxicity in instestine specific-deficient mice. Journal of Lipid Research. 2014; 55:455–465. [PubMed: 24343899]

[9]. Masuno H, Ikura T, Morizono D, Orita I, Yamada S, Shimizu M, Ito N. Crystal structures of complexes of vitamin D receptor ligand-bindig domain with lithocholic acid derivatives. J. Lipid Res. 2013; 54:2206–2213. [PubMed: 23723390]

[10]. Belorusova AY, Eberhardt J, Potier N, Stote RH, Dejaegere A, Rochel N. Structural insights into the molecular mechanisms of vitamin D receptor activation by lithocholic acid involving a new mode of ligand recognition. J. Med. Chem. 2014; 57:4710–4719. [PubMed: 24818857]

[11]. Adachi R, Homna Y, Masuno H, Kawana K, Shimomura I, Yamada S, Makishima M. Selective activation of vitamin D receptor by lithocholic acid acetate, a bile acid derivative. J. Lipid Res. 2005; 46:46–57. [PubMed: 15489543]

[12]. Ishizawa M, Matsunawa M, Adachi R, Uno S, Keda K, Masuno H, Shimizu M, Iwasaki KI, Yamada S, Makishima M. Lithocholic acid derivatives act as selective vitamin D receptor modulators without inducing hypercalcemia. Journal of Lipid Research. 2008; 49:763–772. [PubMed: 18180267]

[13]. Tanaka Y, Castillo L, Deluca HF. The 24-hydroxylation of 1,25-dihydroxyvitamin $D_3$. J. Biol. Chem. 1977; 252:1421–1424. [PubMed: 838723]

[14]. Sakaki T, Sawada N, Komai K, Shiozawa S, Yamada S, Yamamoto K, Ohyama Y, Inouye K. Dual metabolic pathway of 25-hydroxyvitamin $D_3$ catalyzed by human CYP24. Eur. J. Biochem. 2000; 267:6158–6165. [PubMed: 11012668]

[15]. Ishizuka S, Ishimoto S, Norman AW. Biological activity assessment of 1 alpha,25-dihydroxyvitamin D3-26,23-lactone in the rat. J Steroid Biochem. 1984; 20:611–615. [PubMed: 6323873]

[16]. Bao BY, Ting HJ, Hsu JW, Lee YF. Protective role of 1 alpha, 25-dihydroxyvitamin D3 against oxidative stress in nonmalignant human prostate epithelial cells. Int J Cancer. 2008; 122:2699–2706. [PubMed: 18348143]

[17]. Miller GJ, Stapleton GE, Hedlund TE, Moffat KA. Vitamin D receptor expression, 24-hydroxylase activity, and inhibition of growth by 1alpha,25-dihydroxyvitamin D3 in seven human prostatic carcinoma cell lines. Clin Cancer Res. 1995; 1:997–1003. [PubMed: 9816072]

[18]. Jackson H, Solaymani-Dodaran M, Card TR, Aithal GP, Logan R, West J. Influence of ursodeoxycholic acid on the mortality and malignancy associated with primary biliary cirrhosis: a population-based cohort study. Hepatology. 2007; 46:1131–1137. [PubMed: 17685473]

[19]. Berendse K, Engelen M, Ferdinandusse S, Majoie CB, Waterham HR, Vaz FM, Koelman JH, Barth PG, Wanders RJ, Poll-The BT. Zellweger spectrum disorders: clinical manifestations in patients surviving into adulthood. J Inherit Metab Dis. 2015

[20]. Ascher B, Hoffmann K, Walker P, Lippert S, Wollina U, Havlickova B. Efficacy, patient-reported outcomes and safety profile of ATX-101 (deoxycholic acid), an injectable drug for the reduction of unwanted submental fat: results from a phase III, randomized, placebo-controlled study. J Eur Acad Dermatol Venereol. 2014; 28:1707–1715. [PubMed: 24605812]

[21]. Iser JH, Dowling H, Mok HY, Bell GD. Chenodeoxycholic acid treatment of gallstones. A follow-up report and analysis of factors influencing response to therapy. N Engl J Med. 1975; 293:378–383. [PubMed: 1152936]

[22]. Bureeva S, Andia-Pravdivy J, Symon A, Bichucher A, Moskaleva V, Popenko V, Shpak A, Shvets V, Kozlov L, Kaplun A. Selective inhibition of the interaction of C1q with immunoglobulins and the classical pathway of complement activation by steroid and triterpenoids sulfates. Bioorg Med Chem. 2007; 15:2489–2498.

[23]. Sobel AE, Spoerri PE. Steryl Sulfates. I. Preparation and Properties. J. Am. Chem. Soc. 1941; 63:1259–1261.

[24]. Iida T, Tazawa S, Ohshima Y, Niwa T, Goto J, Nambara T. Analysis of conjugated bile acids in human biological fluids. Synthesis of hyodeoxycholic acid 3- and 6-glycosides and related compounds. Chem. Pharm. Bull. 1994; 42:1479–1484. [PubMed: 7923472]

[25]. Becker B, Barua AB, Olsen JA. All-trans-retinoyl B-glucuronide: new procedure for chemical synthesis and its metabolism in vitamin A-deficient rats. Biochem J. 1996; 314:249–252. [PubMed: 8660290]

[26]. Nandhikonda P, Lynt WZ, McCallum MM, Ara T, Baranowski AM, Yuan NY, Pearson D, Bikle DD, Guy RK, Arnold LA. Discovery of the first irreversible small molecule inhibitors of the interaction between the vitamin D receptor and coactivators. J Med Chem. 2012; 55:4640–4651. [PubMed: 22563729]

[27]. Teichert A, Arnold LA, Otieno S, Oda Y, Augustinaite I, Geistlinger TR, Kriwacki RW, Guy RK, Bikle DD. Quantification of the vitamin D receptor-coregulator interaction. Biochemistry. 2009; 48:1454–1461. [PubMed: 19183053]

[28]. Teske K, Nandhikonda P, Bogart JW, Feleke B, Sidhu P, Yuan N, Preston J, Goy R, Arnold LA. Modulation of Transcription mediated by the Vitamin D Receptor and the Peroxisome Proliferator-Activated Receptor delta in the presence of GW0742 analogs. J Biomol Res Ther. 2014; 3

[29]. Northfield TC, McColl I. Postprandial concentrations of free and conjugated bile acids down the length of the normal human small intestine. Gut. 1973; 14:513–518. [PubMed: 4729918]

[30]. Esvelt RP, Schnoes HK, DeLuca HF. Isolation and characterization of 1 alpha-hydroxy-23-carboxytetranorvitamin D: a major metabolite of 1,25-dihydroxyvitamin D3. Biochemistry. 1979; 18:3977–3983. [PubMed: 486408]

[31]. Rochel N, Wurtz JM, Mitschler A, Klaholz B, Moras D. The crystal structure of the nuclear receptor for vitamin D bound to its natural ligand. Mol Cell. 2000; 5:173–179. [PubMed: 10678179]

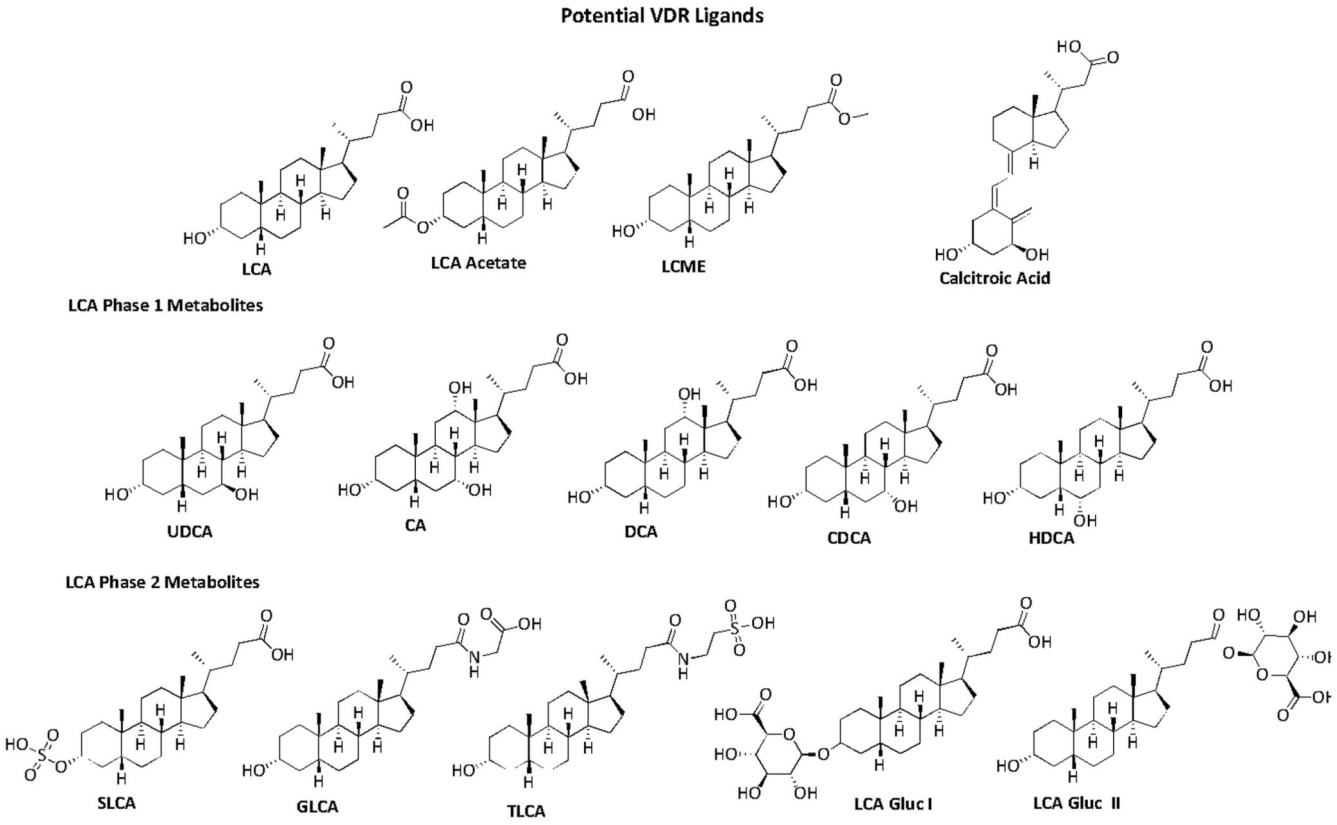


**Figure 1. Summary of the potential natural VDR ligands**

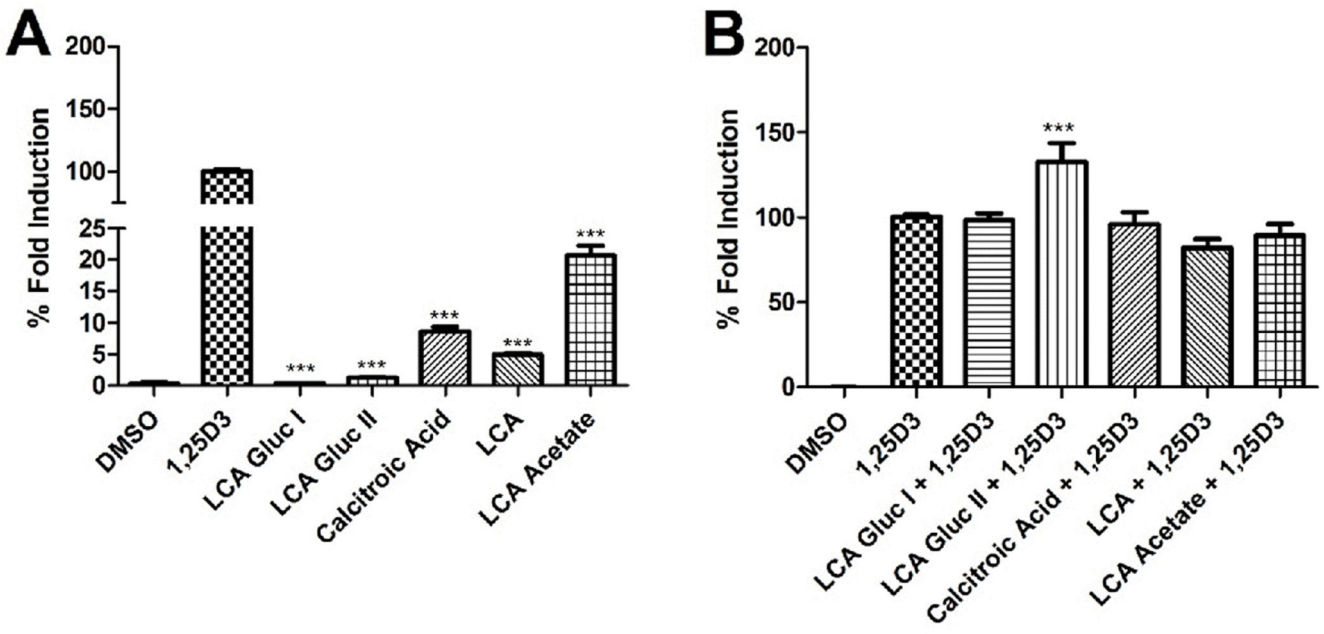


**Figure 2.**

A) CYP24A1 gene regulation by VDR ligands (7.5 μM) in DU145 cells after 18 hours. Stars represent $P < 0.001$ (***) compared to vehicle DMSO. B) CYP24A1 gene regulation by VDR ligands (7.5 μM) in DU145 in the presence of 20 nM $1,25(OH)_2D_3$ after 18 hours. Stars represent $P < 0.001$ (***) compared to $1,25(OH)_2D_3$. All values represent standard errors of mean calculated from three biological independent experiments performed in triplicate. All significance values were determined using ANOVA (Dunnett's comparison test).

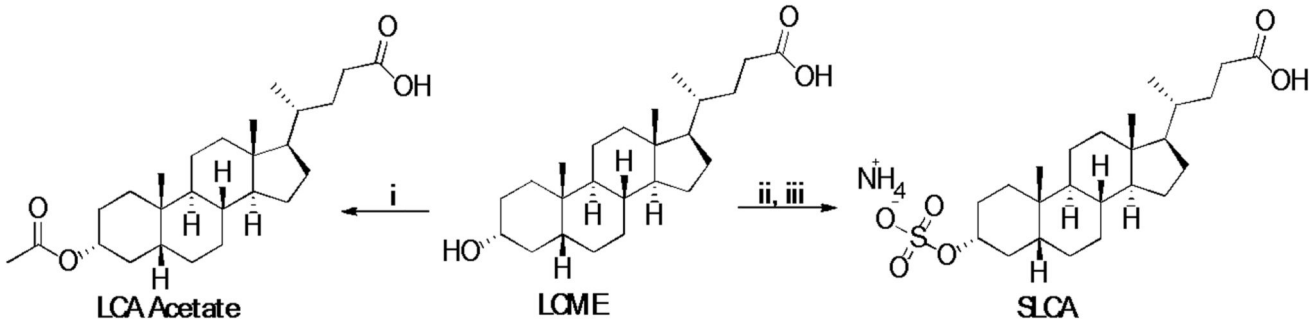


**Scheme 1. Conversion of LCA to LCA acetate and SLCA**

i) Pyridine, acetyl chloride, cat. 4-DMAP, rt, 1 h; ii) sulfuric acid, acetic anhydride, pyridine, 50-55°C, 30 min. iii) 25% ammonia in water, 0°C, 15 min.

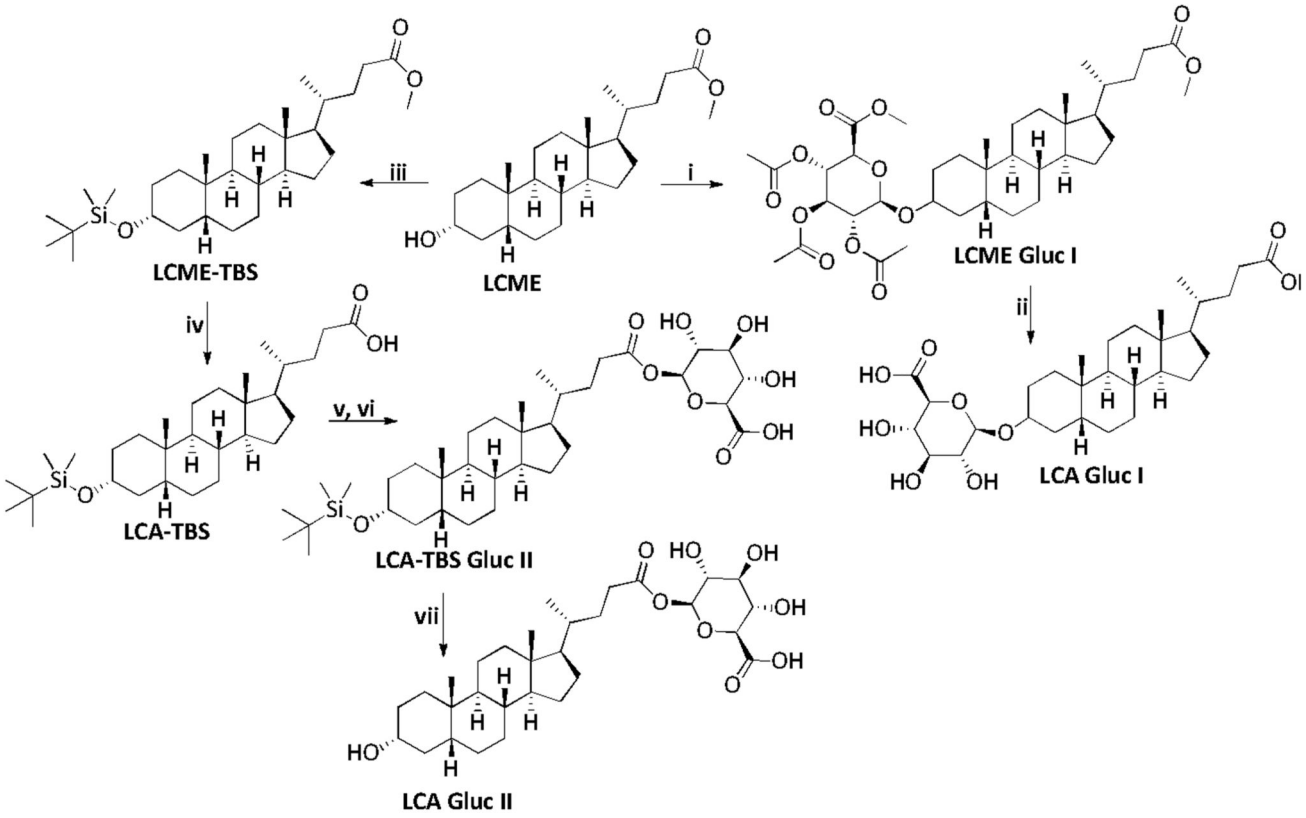


**Scheme 2. Synthetic scheme for converting LCME to LCA *O*-glucuronide I and II**

i) Dry benzene, $CdCO_3$, acetobromo-α-D-glucuronic acid methyl ester, reflux, 5 h; ii) MeOH, 1M NaOH, rt, 4 h followed by 5% HCl; iii) TBDMSCl, DMF, imidazole, rt; iv) THF, 2M NaOH, 75°C, 24 h followed by 2M HCl; v) pyridine, CDI, reflux, 3 h; vi) a) NaH, tetrabutylammonium glucuronate, 50°C, 4-5 h; b) acetic acid; vii) THF, tetrabutylammonium fluoride, 40°C, $H_2O$.

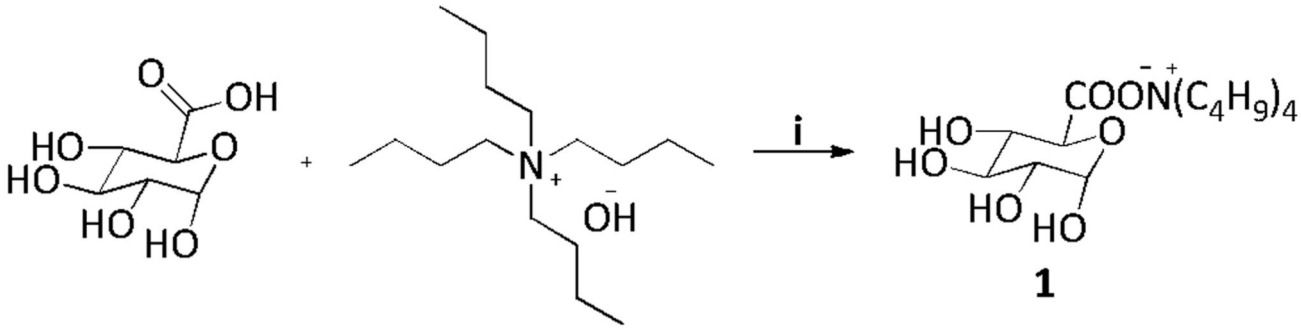


**Scheme 3. Tetrabutylammonium salt (1) formation of glucuronic acid**
i) MeOH, 40°C, 1 h.

## Table 1

Summary of VDR-mediated activities of cholesterol and vitamin D metabolites

| Com-pound | VDR-SRC2-3 Activation $EC_{50}$ (μM)[a] | VDR-SRC2-3 Inhibition $IC_{50}$ (μM)[a] | VDR 2-Hybrid $EC_{50}$ (μM)[b] | VDR 2-Hybrid $IC_{50}$ (μM)[c] | Toxicity $LD_{50}$ (μM)[d] |
|---|---|---|---|---|---|
| **LCA** | >50 | 13.6 ± 4.6 | 2.14 ± 1.03 (39%) | 46.7 ± 8.4 | 55.9 ± 6.5 |
| **LCME** | >150 | >150 | >150 | 15.1 ± 5.1 | 50.4 ± 12.0 |
| **LCA Acetate** | >150 | 11.0 ± 3.2 | 1.49 ± 0.65 (94%) | >50 | >50 |
| **Calcitroic Acid** | >100 | 2.29 ± 0.43 | 0.87 ± 0.29 (55%) | >100 | >100 |
| **UDCA** | >150 | >150 | >150 | >50 | >150 |
| **CA** | >150 | >150 | >150 | >150 | >150 |
| **DCA** | >150 | >150 | >150 | >50 | >150 |
| **CDCA** | >150 | >150 | >150 | >50 | >150 |
| **HDCA** | >150 | >150 | >150 | >50 | >150 |
| **TLCA** | >150 | 14.5 ± 4.3 | >150 | >50 | >150 |
| **GLCA** | >150 | 40.1 ± 8.0 | >150 | >50 | >150 |
| **SLCA** | >150 | 23.3 ± 5.5 | >150 | >50 | >150 |
| **LCA Gluc I** | >50 | 31.5 ± 7.2 | 20.5 ± 13.1 (49%)<br>12.3 ± 3.9 (55%)[e] | >150 | >150 |
| **LCA Gluc II** | >150 | 2.86 ± 0.55 | 6.52 ± 2.61 (29%)<br>21.3 ± 8.0 (70%)[e] | >150 | >150 |

Table 1 is divided into three sections by bolds lines: known VDR ligands, phase 1 metabolites and phase 2 metabolites.

[a] Fluorescence polarization at 635/685 nm with VDR-LBD (0.1 μM), Alexa Fluor-SRC2-3 (7 nM), with and without VDR-agonist LG190178 (0.75 μM). $EC_{50}$ and $IC_{50}$ values were obtained by non-linear regression (Y = Bottom + (Top − Bottom)/(1 + 10(logIC50−X)(HillSlope)) using two independent experiments in quadruplet. The maximum concentration used was 450 μM.

[b] Two-hydrid assay in HEK293T cells using VP16-VDR-LBD, SRC1-GAL4, and luciferase reporter plasmid vector with a 4×UAS repeat with or without 10 nM $1,25(OH)_2D_3$. Efficacy, shown in parenthesis was calculated in respect to full activation with 10 nM $1,25(OH)_2D_3$.

[c] Two-hydrid assay in HEK293T cells using VP16-VDR-LBD, SRC1-GAL4, and luciferase reporter plasmid vector with a 4×UAS repeat in the presence of 10 nM $1,25(OH)_2D_3$.

[d] Treated HEK293 evaluated with Cell-TiterGlo (Promega);

[e] Transcription assay using a hVDR-Gal4 plasmid and a luciferase reporter plasmid containing a 4×UAS repeat.